Applied Catalysis B: Environmental 329 (2023) 122553

Contents lists available at ScienceDirect

Applied Catalysis B: Environmental

journal homepage: www.elsevier.com/locate/apcatb

Electrochemical activation of graphite electrode for nitrate reduction: Energetic performance and application potential

Wenda Kang [a,b,1], Liming Yan [a,1], Jiahao Tang [a], Shuai Wu [a,c], Hongtao Yu [a,*], Zhangliang Li [b,**]

[a] Key Laboratory of Industrial Ecology and Environmental Engineering (Ministry of Education), School of Environmental Science and Technology, Dalian University of Technology, Dalian 116024, China
[b] Fujian Provincial Key Laboratory of Ecology-Toxicological Effects & Control for Emerging Contaminants, College of Environmental and Biological Engineering, Putian University, Putian 351100, China
[c] Center for Water and Ecology, State Key Joint Laboratory of Environment Simulation and Pollution Control, School of Environment, Tsinghua University, Beijing 100084, China

ARTICLE INFO

Keywords:
Nitrate reduction
Graphite electrode
Electrochemical activation
Stability
Scale-up application

ABSTRACT

Electrocatalysis is a potential technology to remove nitrate from wastewater. However, developing an efficient electrode with long-term stability is still a great challenge. Herein, we reported a facile electrochemical activation method to improve nitrate reduction ability of graphite electrodes. Results of cyclic voltammetry and electrochemical impedance spectroscopy showed that the nitrate reduction activity was enhanced and the solid-liquid interfacial resistance was decreased. The activated electrode displayed nitrate reduction rate of 0.0409 min^{-1}, which was 10.8 times that of pristine graphite and closed to Fe and Cu electrodes. Furthermore, taking solution including 50.0 mg/L nitrate-N as target, the activated electrode performed above 90.0 % of nitrate removal during 81 days of continuous running. When activated graphite electrode was enlarged to 2500.0 cm^2, its performance in nitrate reduction was maintained well. These results suggested electrochemical activated graphite electrode was a promising alternative in the real application of nitrate removal from water and wastewater.

1. Introduction

Nitrate pollution in wastewater is becoming more and more serious, which has caused serious harm to environment and human health [1]. So far, many physical [2], chemical [3], and biological techniques [4] have been developed for nitrate remediation, which require strict conditions and complex procedures. In contrast, electrochemical technology using electrons as reducing agents is considered to be a promising technology [5].

The focus of electrochemical technology for the reduction of nitrate is developing an efficient and selective electrode [6]. Nowadays, three types of electrodes have been reported. The first category is metal electrodes [7], such as Sn (263 ¥/kg), Sb (64 ¥/kg), Rh (3.4×10^6 ¥/kg), Pd (4.8×10^5 ¥/kg), Pt (2.3×10^5 ¥/kg), Pb (13.1 ¥/kg), Au (3.7×10^5 ¥/kg), Ag (5.2×10^3 ¥/kg) and so on. Although metal electrodes exhibit excellent electrocatalytic performance, their application is limited by high cost or metal ions leaching. The second category is carbon supported metal electrodes [8]. Using various carbon materials as a carrier can effectively reduce the amount of precious metals, but these composited electrodes still suffer from metal ions leaching. The third category is carbon electrodes, including graphite [9], boron-doped diamond [10], carbon felt [11,12] and charcoal block [13], etc. Because of the merits of low cost and excellent stability, carbon material cathodes have attracted more and more attention for electrochemical reduction of nitrate [14]. However, the performance of carbon materials for electrochemical reduction of nitrate is still far from satisfactory due to the low removal rate of nitrate reduction and the low selectivity of products [15,16]. Different approaches, such as introducing dopants and defects, have been developed to enhance the performance of carbon catalysts for nitrate reduction. However, complex and time-consuming processes are generally needed to fabricate modified carbon materials. Additionally, the fabricated carbon powders are generally attached on

* Correspondence to: Dalian University of Technology, Environmental Building, Room B303, Dalian 116024, China.
** Correspondence to: Putian University, Heyi Building, Room 107, Putian 351100, China.
E-mail addresses: yuhongtao@dlut.edu.cn (H. Yu), ptulizhangliang@126.com (Z. Li).
[1] These authors contributed equally to this work.

https://doi.org/10.1016/j.apcatb.2023.122553
Received 24 November 2022; Received in revised form 1 February 2023; Accepted 28 February 2023
Available online 2 March 2023

the surface of conductive substrates using Nafion as binders, which result the poor stability of the electrode during the continuous operation because the binders may age and carbon powders might peel from the conductive substrates. Therefore, it is urgent to develop a facile method to improve the performance of carbon electrode.

Recently, a novel study found that Ni electrodes may be activated after consecutive cycles during nitrate reduction reaction, exhibiting outstanding performance in nitrate-to-ammonia conversion [17]. Inspired by this study, we explored electrochemical activation of graphite electrode, which could be facilely in-situ activated by electrochemical treatment. In this paper, we identified key influence factors on electrochemical activation of graphite, revealed the mechanism of activation process, and proposed the feasibility and application potential of this method. It is hoped to provide an alternative electrode material for electrochemical nitrate reduction.

2. Experimental

2.1. Materials and chemicals

Graphite was purchased from Graphite Carbon Processing Plant, China. Sodium nitrate ($NaNO_3$), sodium sulfate anhydrous (Na_2SO_4), sulfamic acid (NH_2SO_3H) and potassium iodide (KI) were provided by Tianjin Damao Chemical Reagent Factory. N-1-Naphthylethylene diamine dihydrochloride ($C_{12}H_{14}N_2{\cdot}2HCl$) and seignette salt ($NaKC_4H_4O_6$) were supplied by Tianjin Guangfu Fine Chemical Research Institute. Phosphoric acid (H_3PO_4) and hydrochloric acid (HCl) were purchased from Tianjin Tianli Chemical Reagent Co., Ltd. Mercury iodide red (HgI_2) was supplied by Shanghai Chemical Reagent Procurement and Supply Station. The above chemicals were analytical grade purity and all solutions in this experiment were prepared using ultrapure water (18.2 MΩ•cm).

2.2. Reactor configuration and experimental procedure

The structure of electrochemical reactor is shown in Fig. 1. Its core components are graphite cathode (5.0 ×5.0 cm) and Pt mesh anode (5.0 ×5.0 cm) and the distance between them is 2 cm. The effective volume of this reactor is 40 mL. DC regulated power supply (0.0–10.0 A) was used to provide the constant current. 0.05 M of Na_2SO_4 was used as the electrolyte and the concentration of NO_3^--N was 50.0 mg/L. The speed of magnetic stirring was set as 500 rpm in the whole reaction process.

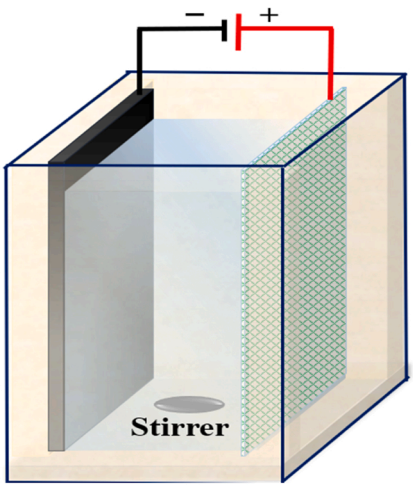

Fig. 1. The structure diagram of the electrochemical reactor.

2.3. Activation process of graphite

The activation process of pristine graphite (5.0 ×5.0 cm) was carried out in a single-chamber reactor with 0.05 M Na_2SO_4 as the electrolyte. The graphite and Pt mesh (the activation process of the scale-up graphite (50.0 ×50.0 cm) used graphite as anode) were acted as cathode and anode, respectively. The activation was stopped after 48, 96, 144, and 192 h under various current densities. In order to distinguish from the pristine graphite, the electrochemically treated electrode was named as activated electrode.

2.4. Calculations

Nitrate-N removal rate (R) was obtained by Eq. (1):

$$R(\%) = \frac{(C_{nitrate-N})_0 - (C_{nitrate-N})_t}{(C_{nitrate-N})_0} \times 100\% \quad (1)$$

Where $(C)_0$ is the initial concentration (mg/L), $(C)_t$ is the concentration (mg/L) at time t (min).

Faradaic efficiency (FE) of nitrate reduction was calculated according to Eq. (2) [18]:

$$FE(\%) = \frac{(C_{nitrate-N})_0 - (C_{nitrate-N})_t}{M \times Q} \times V \times n \times F \times 100\% \quad (2)$$

Where V is cell volume (L), n is electron number involved in the reduction of nitrate to ammonia (8), F is Faraday constant (96,485 C/mol), M is molar mass of nitrogen (14 g/mol), Q is total electrical charge (C) consumed during electrolysis.

2.5. Analytical methods

Nitrate-N and nitrite-N were measured using ultraviolet-visible absorption spectrum according to Chinese National Standard method (HJT346-2007) and (GB7493-1987), respectively. Ammonia-N (in solution or gas phase) was measured by Nessler's reagent spectrophotometry (HJ 535-2009). The above methods were all based on ultraviolet visible spectrophotometer (SP-756 P, Shanghai Spectrum Instrument Co., Ltd.). pH value was tested with a pH meter (FE20K, Mettler Toledo International Trading (Shanghai) Co., Ltd). Total organic carbon (TOC) was measured using a total organic carbon analyzer (Multi N/C2100S, Analytik Jena AG, Germany). The turbidity was tested by turbidimeter (WGZ-200, Shanghai, China). Concentration of metal ions was measured by a plasma emission spectrometer (ICP, Optima2000DV03030429, Perkinelmer). An electron paramagnetic resonance spectrometer (EPR, A200-9.5/12, Bruker) was employed for the semi-quantitative analysis of H* . Cyclic voltammetry (CV) was carried out to investigate the electrochemical performance of the electrode for oxygen reduction at a scan rate of 20.0 mV/s. The linear sweep voltammetry (LSV) and CV were performed using an electrochemical station (ZAHNERZENNIUM, Germany). Electrochemical impedance spectroscopy (EIS) was conducted, and the frequency domain was from 10^{-2} Hz to 10^6 Hz. A three-electrode system was set up using pristine/activated graphite electrode, Pt mesh, and saturated calomel electrode (SCE) as the working electrode, counter electrode, and reference electrode, respectively. The chemical composition was detected by X-ray photoelectron spectrometry with a monochromatized Al X-ray source (XPS, Thermo Scientific, K-Alphα+).

3. Results and discussion

3.1. Activation of graphite electrode and nitrate reduction performance

Electrochemically activated graphite was discovered by an accidental experiment. At that time, after 48 h of continuous electroreduction nitrate experiment, the graphite electrode was used again, and

the concentration of nitrate-N in effluent decreased significantly. To determine this phenomenon, we designed several experiments to identify the main parameters that determined this particular phenomenon. First of all, graphite was placed as cathode in a single-chamber reactor and activated at various current densities (0.4 mA/cm^2, 4.0 mA/cm^2, and 16.0 mA/cm^2) for 48 h or more times (2 times means 96 h, 3 times means 144 h, 4 times means 192 h). Then nitrate removal performance of the activated graphite electrode was investigated at a current density of 4.0 mA/cm^2. As shown in Fig. 2a, for solution with 50.0 mg/L nitrate-N, 37.0 mg/L nitrate-N remained in effluent after 90 min of electrochemical reaction for pristine graphite electrode, which had a low reduction performance on nitrate. For the activated graphite electrode with 48-hour activation at current densities of 0.4 mA/cm^2, 4.0 mA/cm^2, and 16.0 mA/cm^2, the concentration of nitrate-N in effluent decreased from 50.0 mg/L to 34.0 mg/L, 17.9 mg/L, and 8.4 mg/L, respectively, and the nitrate removal performance of activated graphite was significantly improved compared to pristine graphite. Furthermore, when the activation times increased to 3 at a current density of 16.0 mA/cm^2, the concentration of nitrate-N in effluent was further reduced to 2.7 mg/L, whose removal rate of nitrate reached 94.6 %. And continuously increased activation times to 4, nitrate-N concentration in effluent only decreased to 2.5 mg/L. Therefore, nitrate reduction performance of the graphite electrode activated three times at current density of 16.0 mA/cm^2 was improved to the optimum value.

The reduction process of nitrate followed the first-order kinetic and the rate constant of activated graphite was calculated to be 0.0409 min^{-1}, which was 10.8 times that of pristine graphite. During the reduction process of nitrate, a series of products could be produced, such as ammonia and nitrite. As shown in Fig. 2b and c, nitrate was mainly reduced to ammonia and only a small amount of nitrite could be detected, and nitrite could hardly be detected in effluent as the reaction time increased to the 90th minute. With the increase of activation current and time, nitrate removal rate of activated graphite gradually increased and finally stabilized above 94.7 %, and the selectivity of ammonia also stabilized at 82.6 % from 65.7 % (Fig. 2d). These results showed that nitrate removal performance and ammonia selectivity of activated graphite were significantly improved compared with pristine graphite.

The performance of graphite electrode was closely related with current and the duration of electrochemical process, indicating that the enhanced performance of graphite was mainly attribute to the electrochemical treatment and electrochemical treatment could activate the graphite electrode in-situ. To further confirm that the improvement of the activity of graphite electrode for nitrate reduction was ascribed to the electrochemical activation, two groups of control experiments were designed to exclude the influence of other ions (NO_3^-) in the solution and the anodic reaction. Graphite was also activated for 144 h at a current density of 16.0 mA/cm^2, but under different activation conditions. For the first group of control experiments, 50.0 mg/L and 0.0 mg/L of nitrate was added into the Na_2SO_4 electrolyte respectively to exclude the influence of NO_3^- anion. In another control experiment, single-chamber and double-chamber reactors were respectively used with Na_2SO_4 electrolyte to exclude the influence of the anodic reaction. As shown in Fig. 3, the nitrate removal rate of activated graphite electrode reached more than 94.0 % under various activation conditions, which proved that the electroreduction reaction directly acted on the graphite cathode and promoted the nitrate reduction performance of activated graphite electrode.

Nitrate removal performance of activated graphite electrode was closely related to applied current, so nitrate removal performance under different reaction current densities was investigated. As shown in Fig. 4a, the concentration of nitrate-N in effluent at 90th minute decreased from 18.7 mg/L to 2.6 mg/L, respectively, when the current density increased from 1.0 mA/cm^2 to 4.0 mA/cm^2. By increasing current density to 18.0 mA/cm^2, the nitrate concentration of effluent was 1.1 mg/L, which was closed to that of the 4.0 mA/cm^2. The main

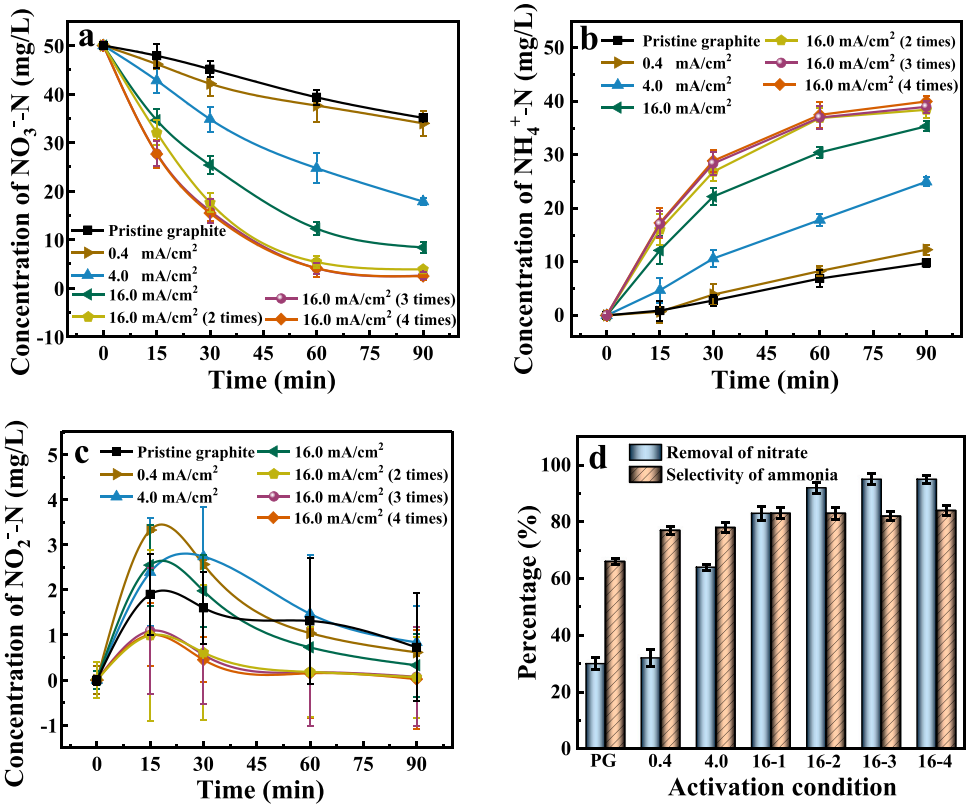

Fig. 2. Concentration of NO_3^--N (a), NH_4^+-N (b) and NO_2^--N (c) in effluent using graphite electrode with various activation conditions and corresponding removal of nitrate/selectivity of ammonia (d). (PG stands for pristine graphite. About 16–1, 16 stands for current density and 1 stands for activation times).

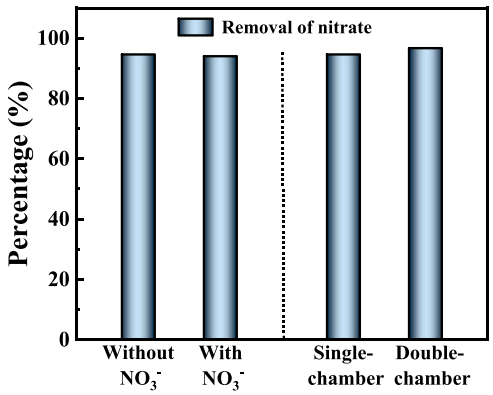

Fig. 3. Effects of NO_3^- ion and anodic reaction on activated graphite electrodes nitrate removal performance during activation process. Double-chamber reactor used PEM membrane.

product of nitrate reduction was ammonia, and the selectivity of ammonia at different current densities was in the range from 77.7 % to 80.5 %. The selectivity of ammonia was relatively stable. Under the condition of high current density, the concentration of ammonia ions decreased after 60 min, because reaction solution was strongly alkaline (pH > 12.0) at this time, and a large number of bubbles were generated on the electrode, which encouraged ammonia ions to escape from solution. As shown in Fig. S1, pH value was 10.2 and 10.8 under 1.0 mA/cm^2 and 2.0 mA/cm^2, respectively, and the ammonia concentration in the gas phase was negligible. As the increase of the applied current density, both pH value and ammonia gas increased gradually. For 18.0 mA/cm^2, pH value and ammonia gas reached 11.3 and 6.1 mg/L, respectively. However, ammonia is a harmful substance in both wastewater and air, so this work further converted the generated ammonia into harmless N_2. It is well known that Cl^- may be oxidized into OCl^- on anode, and OCl^- may oxidize NH_4^+ into harmless N_2. Therefore, in order to eliminate the generated ammonia, we added NaCl to the solution. As shown in Fig. S2a, when NaCl concentration increased from 0.0 g/L to 1.0 g/L, ammonia declined rapidly in effluent. And the ammonia was almost undetectable in the effluent at the 90th minute when the concentration of NaCl was 2.0 mg/L. In addition, the ammonia concentration in the gas phase was detected under various concentrations of NaCl. As shown in Fig. S2b, when the solution without NaCl, the ammonia concentration in the gas phase was 0.3 mg/L. This indicated that some of the ammonia escaped from the solution. Continuing to increase the concentration of NaCl in the solution to 1.0 mg/L, ammonia was undetectable in the gas phase. Nitrite was another product of nitrate reduction. As reaction time increased, the concentration of nitrite in solution first increased and then decreased, and the final concentration of nitrite-N was less than 2.0 mg/L at the 90th minute (Fig. 4c). Although the concentration was low, nitrite was still a toxic by-product. Surprisingly, when the current density was 4.0 mA/cm^2, nitrite was almost undetectable in effluent at the 90th minute. In addition, Faradaic efficiency decreased significantly with the increased of current density (Fig. 4d). Therefore, after comprehensive consideration, current density of 4.0 mA/cm^2 was selected as the optimal condition for subsequent experiments.

Furthermore, the performance of activated graphite electrode for nitrate reduction was compared with that of Fe mesh and Cu mesh under the same experimental conditions. As shown in Fig. 5a, the concentration of nitrate-N in effluent treated by activated graphite electrode (2.7 mg/L) was close to that of Fe mesh (0.7 mg/L) and Cu mesh (3.9 mg/L). And the kinetic rate constants of Fe mesh, Cu mesh, and activated graphite electrode were 0.0414 min^{-1}, 0.0293 min^{-1}, and 0.0409 min^{-1}, respectively. This result demonstrated the activated

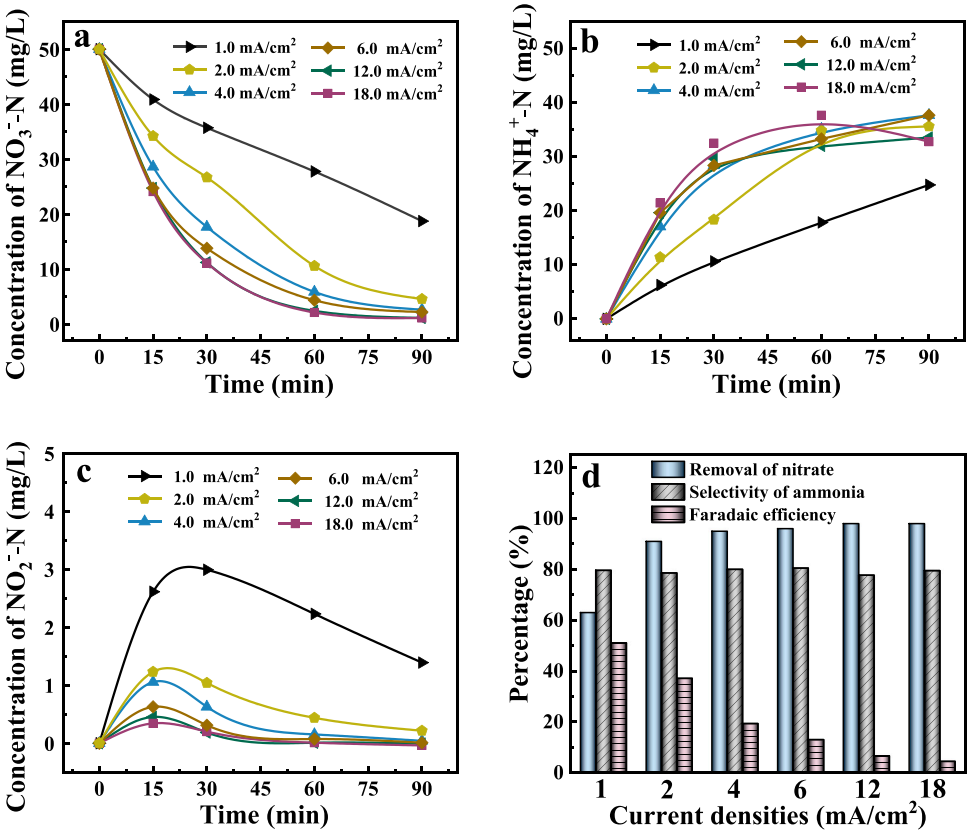

Fig. 4. Concentration of NO_3^--N (a), NH_4^+-N (b) and NO_2^--N (c) in effluent using activated graphite electrode under various reaction current densities and corresponding removal of nitrate/selectivity of ammonia/faradaic efficiency (d).

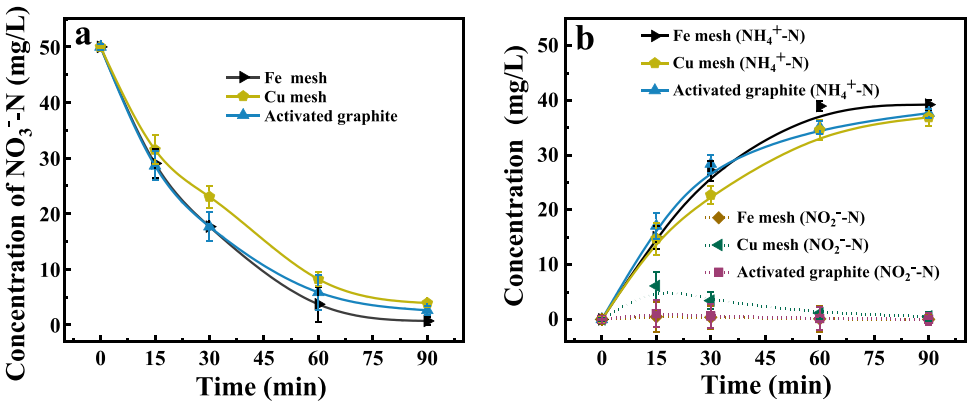

Fig. 5. Concentration of NO_3^--N (a), NH_4^+-N and NO_2^--N (b) in effluent using Fe mesh, Cu mesh and activated graphite electrode.

graphite without metal loading exhibited competitive performance with metal electrodes, highlighting the promising application of activated graphite electrode. The concentrations of ammonia and nitrite in effluent treated by three electrodes showed the same trend (Fig. 5b). On basis of the Eqs. (S1–S3), we calculated energy consumption, selectivity of ammonia, and selectivity of nitrite of activated graphite electrode to be 0.332 kWh/g nitrate-N, 80.2 %, and 0.1 %, respectively, which were very similar to those of metal electrodes (Table S1). Then, concentration of metal ions in the solution after electrochemical reaction was measured. The concentrations of Fe ion and Cu ion in effluent treated by Fe, Cu mesh electrode were 3.6 mg/L and 0.8 mg/L, respectively. In contrast to the above metal electrodes, no metal ion was detected in effluent treated by activated graphite electrode, indicating that there was no issue of metal leaching for activated graphite electrode. Further, considering the possibility of carbon leaching or precipitation, the total organic carbon (TOC) and turbidity of the effluent were tested. The results showed that the value of TOC and turbidity of the effluent increased to 0.5 mg/L and 0.3 NTU, respectively, so it is believed that some organic carbon particles leached from the graphite electrode into the solution during the reaction. However, due to the high values of TOC in the actual water, the value of leached organic carbon in this job was negligible. The above results proved that activated graphite electrode exhibited comparable performance with metal electrode, but avoided the problem of metal leaching.

3.2. Mechanism of activated graphite for nitrate reduction

To better understand the nitrate reduction mechanism of activated graphite electrode, the variation of solution pH during the reaction was monitored. As shown in Fig. 6, pH of the solution treated by activated graphite electrode reached 10.8 at the 15th minute, and then slowly increased to 11.1 at the 90th minute. However, solution pH treated by pristine graphite electrode rose to 10.5 at the 30th minute, and decreased to 10.3 at the 90th minute. The above results were consistent with the nitrate reduction activity of pristine and activated graphite electrodes. It could be rationally deduced that activated graphite electrode exhibited higher reactivity for nitrate reduction and consumed H^+ faster.

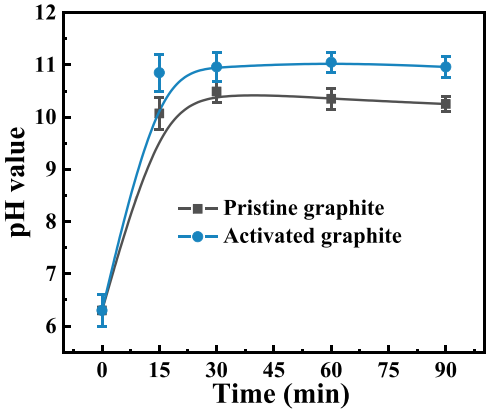

Fig. 6. pH variation trend during the reaction of pristine and activated graphite electrode.

To further uncover the mechanism of electrochemical reduction of nitrate over activated graphite electrode, EPR and electrochemical characterizations were performed. According to previous reports, nitrate reduction occurs through two pathways, that is atomic H* mediated process and direct electron transfer [19,20]. EPR test was firstly performed to reveal the reaction pathway of activated graphite electrode for nitrate reduction. Because EPR was sensitive to the species with unpaired electrons, atomic H* with unpaired electron could be detected immediately if atomic H* was produced. As shown in Fig. 7a, characteristic nine-line peaks attributed to DMPO−H did not appear in pristine and activated graphite systems, indicating that no atomic H* was produced on pristine or activated graphite cathode. Therefore, it could be deduced that H* mediated process did not play a dominant role on the reduction of nitrate during the electrochemical process and direct electron reduction would be the main pathway for the electrochemical reduction of nitrate. This result is consistent with previous reports that H* mediated process generally occurs on the noble metal electrodes while carbon electrodes are inclined to follow the direct electron transfer pathway [17,21].

To further demonstrate the important role of direct electron transfer for nitrate reduction, various electrochemical characterizations were performed. CV test showed that electroactive surface area of the activated graphite electrode was larger than that of pristine graphite electrode (Fig. 7b). When 50.0, 200.0 and 500.0 mg/L nitrate-N were added to reaction solution, the peaks current appeared at the cathode potential of activated graphite electrode at − 0.5 V. These reduction peaks can be attributed to electron transfer from the cathode to nitrate, since no peak was observed in the absence of nitrate. Fig. 7c showed the variation trend of response current intensity observed in LSV measurement. The current density generated by activated graphite electrode was significantly stronger than that of pristine graphite electrode, indicating that activated graphite electrode displayed stronger ability for nitrate reduction. In addition, with the increased of nitrate-N concentration in electrolyte, the current density of the activated graphite electrode increased significantly, indicating that nitrate reduction was more kinetically favorable on activated electrode [22]. EIS was further used to explore the electrochemical performance of the electrode (Fig. 7d). The radius of the semicircle was related to the charge transfer resistance, and the smaller the radius of the semicircle, the faster the electron transfer at the interface [23]. The dramatically decreased semicircle of the

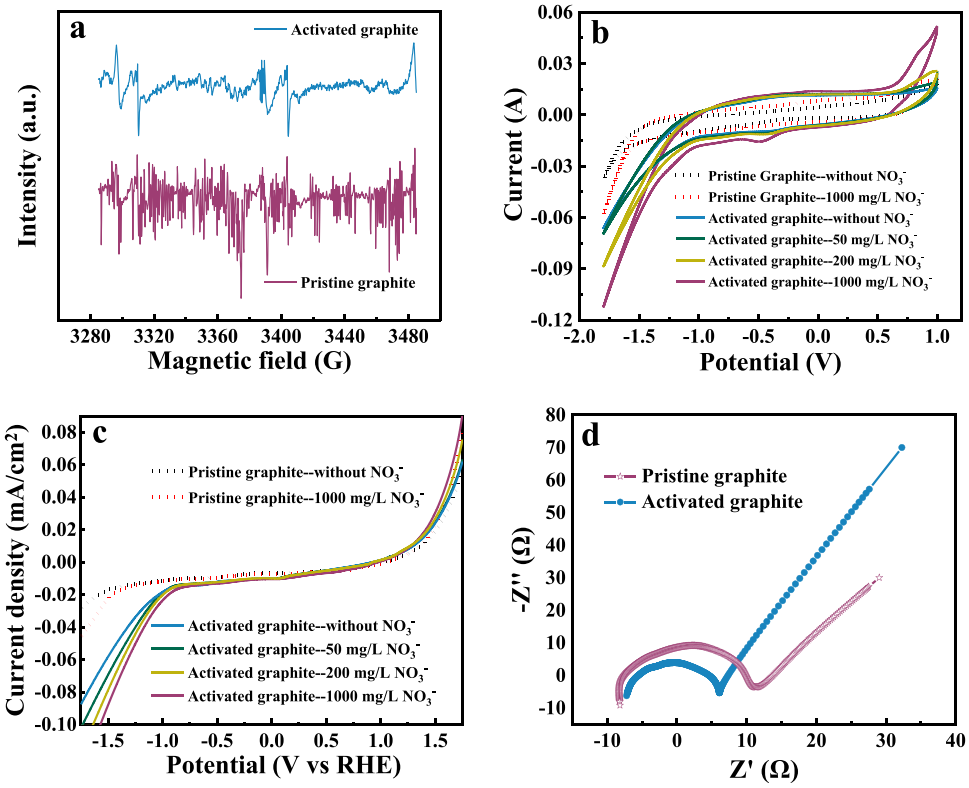

Fig. 7. (a) EPR spectra of pristine and activated graphite; (b) CV curves of nitrate reduction by pristine and activated graphite electrode at a scan rate of 20 mV/s; (c) LSV curves of different electrolytes at a scan rate of 40 mV/s; (d) EIS Nyquist plots of the pristine/activated graphite by applying an impedance amplitude of 10 mV with the frequency range from 10^{-2} Hz to 10^{6} Hz.

activated electrode revealed that rapid electron transfer between nitrate and the activated electrode could be achieved. It was concluded that reduced solid-liquid interfacial resistance of activated graphite electrode was the main reason for the improvement of nitrate reduction performance.

Finally, the functionalization degree of activated graphite after electrochemical treatment was determined by XPS analysis. The C1s peaks of the pristine/activated graphite electrode showed that the peaks fitted four Lorentz functions well, corresponding to four carbon states with different binding energies (Fig. 8a): C-C (284.5 eV), defective carbon (285.4 eV), O═C-OH (288.5 eV), and a π-π form of graphite material (291.2 eV) [24]. The obvious difference was that the defective carbon content of activated graphite was higher than that of the pristine graphite electrode. According to a literature [25], the defective carbon may improve the electrocatalytic performance by changing the surface charge state and adjusting the adsorption free energy of the key intermediates. According to the high-resolution XPS spectrum of O1s peaks from activated graphite (Fig. 8b), the surface of activated graphite was rich in oxygen containing functional groups such as C═O at 531.6 eV and C–O at 533.2 eV. The abundance of oxygen containing functional groups indicated that the surface of the graphite was modified and therefore more defects were formed [26], which may beneficial for the electron transfer and improve the performance for nitrate reduction.

In addition, SEM image and AFM photograph showed the morphological changes occurring on the surface of the electrode. As shown in Fig. S3, the surface of the activated electrode was rougher than that of the pristine electrode. And the AMF photograph (Fig. S4) also proved that the average roughness of the activated electrode (Ra=199.3) was higher than that of the pristine electrode (Ra=149.4), which may expose more active sites on the surface of the activated graphite electrode.

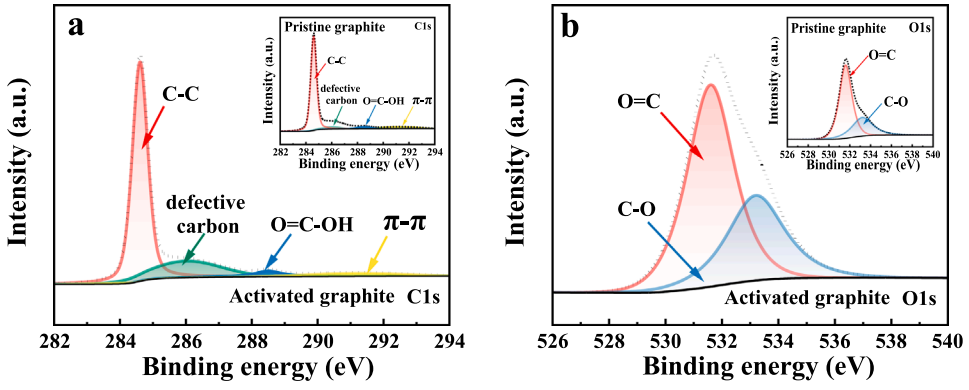

Fig. 8. High-resolution XPS spectrum of (a) C1s peaks and (b) O1s peaks from activated/pristine graphite.

3.3. Stability and scale-up performance of activated graphite

Long-term stability is the key metric for the practical application of electrochemical reduction of nitrate. To evaluate the stability of activated graphite electrode, a continuous flow reactor was designed and activated graphite (5.0 cm × 5.0 cm) was assembled into the reactor as shown in Fig. 9a to investigate the performance of nitrate reduction. By setting the flow rate of flow pump, the hydraulic retention time of the solution in the continuous flow reactor was controlled to be 90 min, and the applied current density was 4.0 mA/cm^2. During the continuous operation, three samples were taken every day to test the concentration of nitrate-N, ammonia-N and nitrite-N, and the average value was calculated as the concentration of nitrogenous ions in the effluent. Before the continuous flow operation, the performance of activated graphite was firstly evaluated in the batch experiment with continuously vigorous stirring. As shown in Fig. 9a, the concentration of nitrate decreased from 50.0 mg/L to 2.8 mg/L as the reaction time increased to 90 min, which was consistent with the results of Figs. 2 and 4. In the continuous flow experiment, the nitrate-N concentration in the effluent decreased to 4.3 mg/L when solution containing 50.0 mg/L of nitrate continuously flowed through the continuous flow reactor. It is worth noting that the concentration of nitrate in the effluent under the continuous flow condition was consistent with that in the batch experiment with continuously vigorous stirring. This result demonstrated that the flow-through electrochemical reactor efficiently promoted the mass transport process and ensured sufficient mixing of substances in the solution, approaching the effect of vigorous stirring in the batch experiment. Surprisingly, the activated graphite displayed a stable operation for nitrate reduction during 81-day of continuous operation with no obvious degradation. The nitrate-N concentration of effluent only slightly fluctuated between 3.0 mg/L and 5.1 mg/L, reflecting the long-term stability of the activated electrode. Then a batch experiment was conducted with the activated electrode that had been used continuously for 81 days. And the nitrate-N concentration of the effluent was 2.5 mg/L, which was close to the value of the first use, further proving the excellent stability of activated electrode. As much as we know, activated electrode exhibited the longest stability (~2000 h) compared with previously reported electrodes for nitrate reduction as shown in Fig. 10a, which was one or two orders of magnitude longer than those of reported electrodes. In addition, the first and the 1500th cycle of CV test were highly coincident (Fig. 10b), which also proved that the activated graphite electrode was stable. The ultra-stable performance was mainly attributed to the self-supporting structure of the activated graphite without polymeric binders and metal loading. The structural integrity and excellent stability suggested the great potential of activated graphite electrode for practical application. In addition, the concentrations of ammonia-N and nitrite-N in the effluent were recorded during 81-day of continuous experiment (Fig. 9b). The ammonia-N concentration fluctuated in the range of 32.0 mg/L and 39.2 mg/L, but the concentration of nitrite-N remained stable below 0.4 mg/L. Further, during 81 days of continuous operation, the voltage fluctuated between 3.9 V and 4.3 V, which led to an energy consumption fluctuating in a small range from 0.325 to 0.343 kWh/g nitrate-N. The result further proved the good stability of the activated graphite electrode.

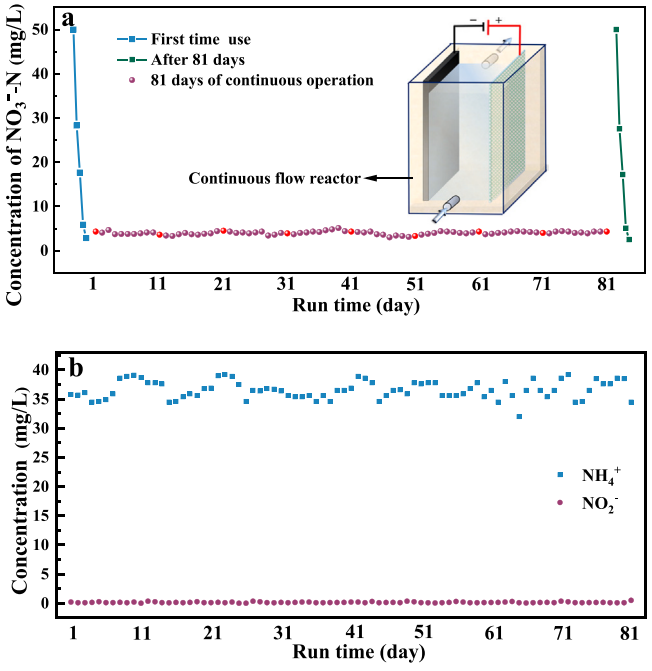

Fig. 9. Concentration of NO_3^--N (a), NH_4^+-N and NO_2^--N (b) in effluent by activated graphite electrode during 81 days of continuous experiment.

Scalability is also an important metric for the application of electrochemical technique. However, traditional powder catalysts are difficult to scale-up because of the elaborate design and complex synthetic process. Electrochemical activation method reported in this work provided a simple and facile approach to promote the performance of carbon electrodes for nitrate reduction. To explore the application potential of activated graphite for nitrate reduction, a scale-up graphite electrode with the size of 50.0 cm × 50.0 cm was activated. The area of the scale-up graphite electrode was 100 times larger than those of previous reported electrodes. The activation conditions adopted the previous optimal parameters, and the anode was replaced with graphite (50.0 cm × 50.0 cm). Subsequently, a scale-up reactor was designed with solution volume of 8 L and electrode area of 2500.0 cm^2 (as shown in Fig. 11a). As much as we know, this is the largest electrode and electrochemical reactor ever reported for nitrate reduction. As shown in Fig. 11b, the concentration of nitrate-N in effluent by the pristine graphite was 34.2 mg/L after 240 min of treatment. In sharp contrast, the effluent nitrate-N concentration of activated graphite electrode decreased to 8.0 mg/L and the reaction rate constant was 0.008 min^{-1}, which was 4.7 times that of the pristine graphite, demonstrating that electrochemical activation process was also efficient even if the area of graphite electrode increased by 100 times. It should be mentioned that the performance of the activated graphite electrode with 2500.0 cm^2 of area slightly decreased compared with the activated graphite electrode with 25.0 cm^2 of area. Therefore, further optimizing the parameters during the scale-up process is needed to improve the performance for nitrate reduction. Even so, the scale-up activated graphite electrode displayed enhanced performance for nitrate reduction and ammonia production. As shown in Fig. 11c, after 240 min of treatment, nitrate was mainly converted into ammonia, and nitrite can hardly be detected in the effluent. Additionally, the selectivity of ammonia (90.1 %) and Faradaic efficiency (12.9 %) of the activated graphite electrode were higher than those of the pristine graphite electrode (Fig. 11d), indicating that the scale-up activated graphite electrode still had good electrochemical denitrification performance.

4. Conclusions

An electrochemical activation method was systematically investigated to improve performance of the graphite electrode for nitrate reduction. Activation process reduced solid-liquid interfacial resistance and increased the defect content of the activated graphite electrode. The nitrate reduction rate constant of activated graphite electrode was increased by an order of magnitude compared with pristine graphite, which was close to those of metal electrodes. The ammonia selectivity and Faradaic efficiency of the activated graphite electrode were also improved. In addition, the activated graphite electrode showed ultra-stable performance up to 2000 h and was easily to scale up (2500.0 cm^2). This study is promising for the practical application of graphite electrode in the field of electroreduction of nitrate.

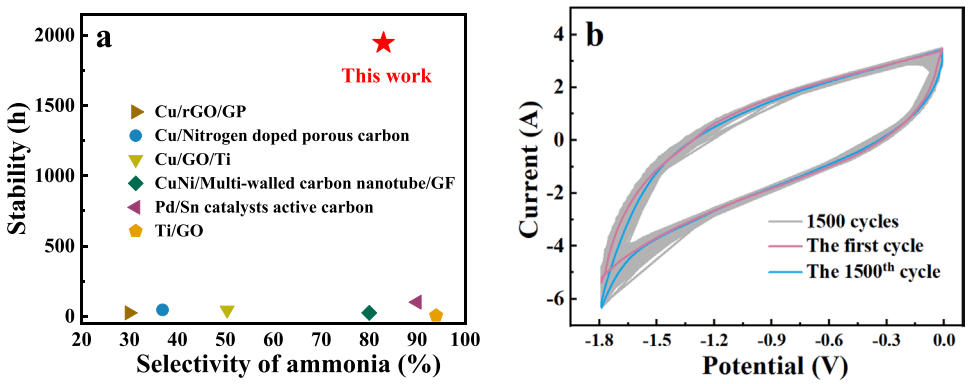

Fig. 10. (a) Stability of activated graphite among carbon-based supported electrodes. Cu/rGO/GP [9], Cu/Nitrogen doped porous carbon [8], Cu/GO/Ti [27], CuNi/Multi-walled carbon nanotube/GF [28], Pd/Sn catalysts active carbon [29], Ti/GO [30]. (b) CV curves of activated graphite electrode for 1500 cycles at a rate of 0.4 V/s in 0.05 M Na_2SO_4 solution.

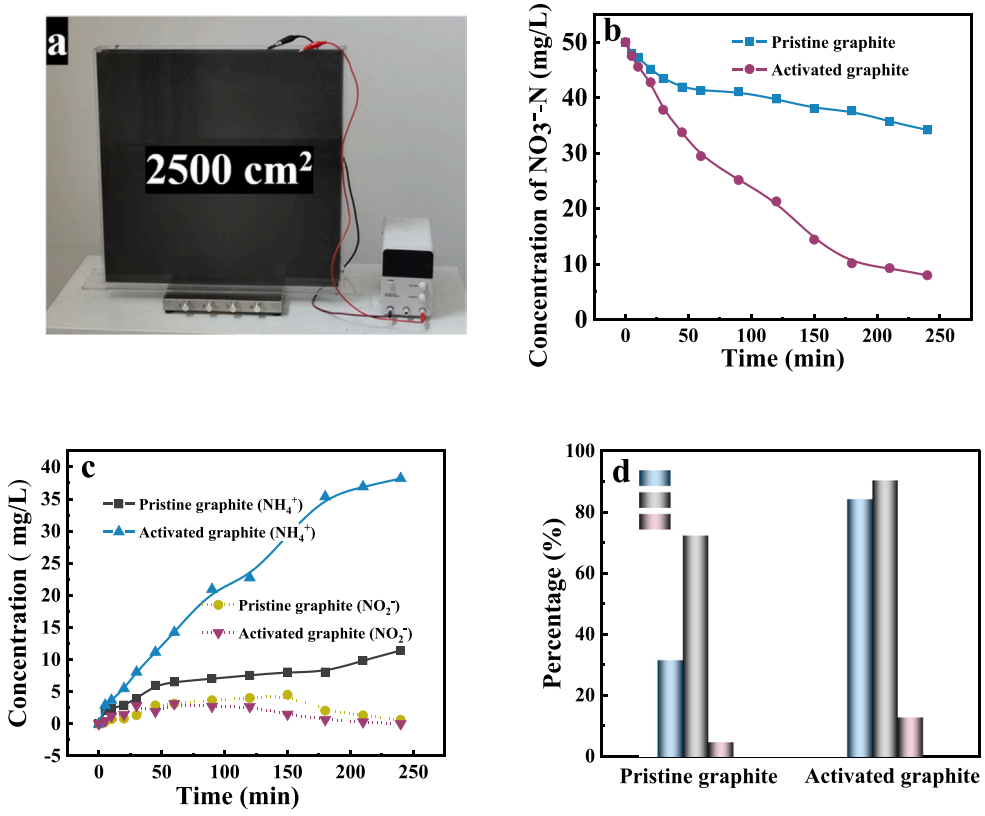

Fig. 11. (a) Real picture of scale-up graphite; Concentration of NO_3^--N (b), NH_4^+-N and NO_2^--N (c) in effluent by scale-up pristine/activated graphite electrode; and corresponding removal of nitrate/selectivity of ammonia/faradaic efficiency (d).

CRediT authorship contribution statement

The authors claim that no conflict of interest exits in the submission of this manuscript, and manuscript is approved by all authors for publication. I would like to declare on behalf of co-authors that the work described is original research that has not been published previously, and not under consideration for publication elsewhere, in whole or in part. All the authors have approved the manuscript.

Declaration of Competing Interest

The authors declare that they have no known competing financial interests or personal relationships that could have appeared to influence the work reported in this paper.

Data availability

Data will be made available on request.

Acknowledgements

This work was financial supported by National Natural Science Foundation of China (No. U22A20241), National Key Research and Development Program of China (2020YFA0211001) and Fujian Provincial Key Laboratory of Ecology-Toxicological Effects & Control for Emerging Contaminants (PY22005).

Appendix A. Supporting information

Supplementary data associated with this article can be found in the online version at doi:10.1016/j.apcatb.2023.122553.

References

[1] C. Jiang, M. Zhang, G. Dong, T. Wei, J. Feng, Y. Ren, T. Luan, Photocatalytic nitrate reduction by a non-metal catalyst h-BN: performance and mechanism, Chem. Eng. J. 429 (2022), 132216, https://doi.org/10.1016/j.cej.2021.132216.

[2] M. Lasagna, D.A. De Luca, E. Franchino, The role of physical and biological processes in aquifers and their importance on groundwater vulnerability to nitrate pollution, Environ. Earth Sci. 75 (2016), https://doi.org/10.1007/s12665-016-5768-1.

[3] J.C. Fanning, The chemical reduction of nitrate in aqueous solution, Coord. Chem. Rev. 199 (2000) 159–179, https://doi.org/10.1016/S0010-8545(99)00143-5.

[4] K. Velusamy, S. Periyasamy, P.S. Kumar, D.N. Vo, J. Sindhu, D. Sneka, B. Subhashini, Advanced techniques to remove phosphates and nitrates from waters: a review, Environ. Chem. Lett. 19 (2021) 3165–3180, https://doi.org/10.1007/s10311-021-01239-2.

[5] Y. Zeng, C. Priest, G. Wang, G. Wu, Restoring the nitrogen cycle by electrochemical reduction of nitrate: progress and prospects, Small Methods 4 (2020) 2000672, https://doi.org/10.1002/smtd.202000672.

[6] X. Zhang, Y. Wang, C. Liu, Y. Yu, S. Lu, B. Zhang, Recent advances in non-noble metal electrocatalysts for nitrate reduction, Chem. Eng. J. 403 (2021), 126269, https://doi.org/10.1016/j.cej.2020.126269.

[7] Y. Ma, J. Chu, Z. Li, D. Rakov, X. Han, Y. Du, B. Song, P. Xu, Homogeneous metal nitrate hydroxide nanoarrays grown on nickel foam for efficient electrocatalytic oxygen evolution, Small 14 (2018), 1803783, https://doi.org/10.1002/smll.201803783.

[8] X. Zhao, K. Zhao, X. Quan, S. Chen, H. Yu, Z. Zhang, J. Niu, S. Zhang, Efficient electrochemical nitrate removal on Cu and nitrogen doped carbon, Chem. Eng. J. 415 (2021), 128958, https://doi.org/10.1016/j.cej.2021.128958.

[9] D. Yin, Y. Liu, P. Song, P. Chen, X. Liu, L. Cai, L. Zhang, In situ growth of copper/reduced graphene oxide on graphite surfaces for the electrocatalytic reduction of nitrate, Electrochim. Acta 324 (2019), 134846, https://doi.org/10.1016/j.electacta.2019.134846.

[10] P. Kuang, K. Natsui, C. Feng, Y. Einaga, Electrochemical reduction of nitrate on boron-doped diamond electrodes: effects of surface termination and boron-doping level, Chemosphere 251 (2020), 126364, https://doi.org/10.1016/j.chemosphere.2020.126364.

[11] W. Zhu, X. Zhang, Y. Yin, Y. Qin, J. Zhang, Q. Wang, In-situ electrochemical activation of carbon fiber paper for the highly efficient electroreduction of concentrated nitric acid, Electrochim. Acta 291 (2018) 328–334, https://doi.org/10.1016/j.electacta.2018.08.127.

[12] J. Ding, W. Li, Q. Zhao, K. Wang, Z. Zheng, Y. Gao, Electroreduction of nitrate in water: role of cathode and cell configuration, Chem. Eng. J. 271 (2015) 252–259, https://doi.org/10.1016/j.cej.2015.03.001.

[13] X. Li, Y. Gu, S. Wu, S. Chen, X. Quan, H. Yu, Selective reduction of nitrate to ammonium over charcoal electrode derived from natural wood, Chemosphere 285 (2021), 131501, https://doi.org/10.1016/j.chemosphere.2021.131501.

[14] E. Lacasa, P. Cañizares, J. Llanos, M.A. Rodrigo, Effect of the cathode material on the removal of nitrates by electrolysis in non-chloride media, J. Hazard. Mater. 213–214 (2012) 478–484, https://doi.org/10.1016/j.jhazmat.2012.02.034.

[15] S. Pu, D. Deng, K. Wang, M. Wang, Y. Zhang, L. Shangguan, W. Chu, Optimizing the removal of nitrate from aqueous solutions via reduced graphite oxide–supported nZVI: synthesis, characterization, kinetics, and reduction mechanism, Environ. Sci. Pollut. Res. 26 (2019) 3932–3945, https://doi.org/10.1007/s11356-018-3813-1.

[16] O. Ghodbane, M. Sarrazin, L. Roué, D. Bélanger, Electrochemical reduction of nitrate on pyrolytic graphite-supported Cu and Pd–Cu electrocatalysts, J. Electrochem. Soc. 155 (2008) F117, https://doi.org/10.1149/1.2900094.

[17] W. Zheng, L. Zhu, Z. Yan, Z. Lin, Z. Lei, Y. Zhang, H. Xu, Z. Dang, C. Wei, C. Feng, Activated Ni cathode for electrocatalytic nitrate reduction to ammonia: from fundamentals to scale-up for treatment of industrial wastewater, Environ. Sci. Technol. (2021), https://doi.org/10.1021/acs.est.1c02278.

[18] Z.A. Jonoush, A. Rezaee, A. Ghaffarinejad, Electrocatalytic nitrate reduction using Fe_0/Fe_3O_4 nanoparticles immobilized on nickel foam: selectivity and energy consumption studies, J. Clean. Prod. 242 (2020), 118569, https://doi.org/10.1016/j.jclepro.2019.118569.

[19] Y. Wang, C. Wang, M. Li, Y. Yu, B. Zhang, Nitrate electroreduction: mechanism insight, in situ characterization, performance evaluation, and challenges, Chem. Soc. Rev. 50 (2021) 6720–6733, https://doi.org/10.1039/D1CS00116G.

[20] M. Duca, M.T.M. Koper, Powering denitrification: the perspectives of electrocatalytic nitrate reduction, Energ. Environ. Sci. 5 (2012) 9726–9742, https://doi.org/10.1039/C2EE23062C.

[21] S. Guo, K. Heck, S. Kasiraju, H. Qian, Z. Zhao, L.C. Grabow, J.T. Miller, M.S. Wong, Insights into nitrate reduction over indium-decorated palladium nanoparticle catalysts, ACS Catal. 8 (2018) 503–515, https://doi.org/10.1021/acscatal.7b01371.

[22] M.H. Dalal, C. Lee, G.G. Wallace, Cathodic exfoliation of graphite into graphene nanoplatelets in aqueous solution of alkali metal salts, J. Mater. Sci. 56 (2021) 3612–3622, https://doi.org/10.1007/s10853-020-05468-8.

[23] J. Gao, B. Jiang, C. Ni, Y. Qi, Y. Zhang, N. Oturan, M.A. Oturan, Non-precious Co_3O_4-TiO_2/Ti cathode based electrocatalytic nitrate reduction: preparation, performance and mechanism, Appl. Catal. B Environ. 254 (2019) 391–402, https://doi.org/10.1016/j.apcatb.2019.05.016.

[24] Y. Zhang, Y. Xu, Simultaneous electrochemical dual-electrode exfoliation of graphite toward scalable production of high-quality graphene, Adv. Funct. Mater. 29 (2019) 1902171, https://doi.org/10.1002/adfm.201902171.

[25] Y. Wu, Y. Gu, W. Kang, H. Yu, S. Chen, X. Quan, N. Lu, Construction of microchannel charcoal cathodes with spatial-constraint capability for enhancing reduction of NO_3^- in high-salinity water, Chem. Eng. J. 452 (2023), 139126, https://doi.org/10.1016/j.cej.2022.139126.

[26] M. Cheng, C. Xiao, Y. Xie, Photocatalytic nitrogen fixation: the role of defects in photocatalysts, J. Mater. Chem. A 7 (2019) 19616–19633, https://doi.org/10.1039/c9ta06435d.

[27] J. Wang, S. Wang, Z. Zhang, C. Wang, Preparation of Cu/GO/Ti electrode by electrodeposition and its enhanced electrochemical reduction for aqueous nitrate, J. Environ. Manag. 276 (2020), 111357, https://doi.org/10.1016/j.jenvman.2020.111357.

[28] C. Lu, X. Lu, K. Yang, H. Song, S. Zhang, A. Li, Cu, Ni and multi-walled carbon-nanotube-modified graphite felt electrode for nitrate electroreduction in water, J. Mater. Sci. 56 (2021) 7357–7371, https://doi.org/10.1007/s10853-020-05764-3.

[29] A.E. Palomares, C. Franch, A. Corma, A study of different supports for the catalytic reduction of nitrates from natural water with a continuous reactor, Catal. Today 172 (2011) 90–94, https://doi.org/10.1016/j.cattod.2011.05.015.

[30] X. Ma, M. Li, X. Liu, L. Wang, N. Chen, J. Li, C. Feng, A graphene oxide nanosheet-modified Ti nanocomposite electrode with enhanced electrochemical property and stability for nitrate reduction, Chem. Eng. J. 348 (2018) 171–179, https://doi.org/10.1016/j.cej.2018.04.168.